Human Molecular Genetics, 2020, Vol. 29, No. 9 1454–1464

doi: 10.1093/hmg/ddaa063
Advance Access Publication Date: 10 April 2020
General Article

GENERAL ARTICLE

Mitochondrial transport mediates survival of retinal ganglion cells in affected LHON patients

Tien-Chun Yang[1,†], Aliaksandr A. Yarmishyn[1,†], Yi-Ping Yang[1,2,3], Pin-Chen Lu[1], Shih-Jie Chou[1,4], Mong-Lien Wang[1,2,3,4], Tai-Chi Lin[3,5], De-Kuang Hwang[3,5], Yu-Bai Chou[3,5], Shih-Jen Chen[3,5], Wei-Kuang Yu[5], An-Guor Wang[3,5], Chih-Chien Hsu[3,5,*,‡,†] and Shih-Hwa Chiou[1,2,5,‡]

[1]Department of Medical Research, Taipei Veterans General Hospital, Taipei 11217, Taiwan, [2]School of Pharmaceutical Sciences, National Yang-Ming University, Taipei 11221, Taiwan, [3]School of Medicine, National Yang-Ming University, Taipei 11221, Taiwan, [4]Institute of Pharmacology, National Yang-Ming University, Taipei 11221, Taiwan and [5]Department of Ophthalmology, Taipei Veterans General Hospital, Taipei 11217, Taiwan

*To whom correspondence should be addressed at: Department of Ophthalmology, Taipei Veterans General Hospital, Taipei 112, Taiwan. Tel: +886-2-28757394; Fax: +886 228732131; Email: chihchienym@gmail.com

Abstract

The mutations in the genes encoding the subunits of complex I of the mitochondrial electron transport chain are the most common cause of Leber's hereditary optic neuropathy (LHON), a maternal hereditary disease characterized by retinal ganglion cell (RGC) degeneration. The characteristics of incomplete penetrance indicate that nuclear genetic and environmental factors also determine phenotypic expression of LHON. Therefore, further understanding of the role of mutant mitochondrial nicotinamide adenine dinucleotide dehydrogenase subunit proteins and nuclear genetic factors/environmental effects in the etiology of LHON is needed. In this study, we generated human-induced pluripotent stem cells (hiPSCs) from healthy control, unaffected LHON mutation carrier, and affected LHON patient. hiPSC-derived RGCs were used to study the differences between affected and unaffected carriers of mitochondrial DNA point mutation m.11778G > A in the *MT-ND4* gene. We found that both mutated cell lines were characterized by increase in reactive oxygen species production, however, only affected cell line had increased levels of apoptotic cells. We found a significant increase in retrograde mitochondria and a decrease in stationary mitochondria in the affected RGC axons. In addition, the messenger RNA and protein levels of KIF5A in the LHON-affected RGCs were significantly reduced. Antioxidant N-acetyl-L-cysteine could restore the expression of KIF5A and the normal pattern of mitochondrial movement in the affected RGCs. To conclude, we found essential differences in the mutually dependent processes of oxidative stress, mitochondrial transport and apoptosis between two LHON-specific mutation carrier RGC cell lines, asymptomatic carrier and disease-affected, and identified KIF5A as a central modulator of these differences.

[†]Chih-Chien Hsu, http://orcid.org/0000-0003-2354-2999
[†]Equal contributions (co-first authors).
[‡]Equal contribution.

Received: October 22, 2019. **Revised:** March 2, 2020. **Accepted:** March 30, 2020

Introduction

Leber's hereditary optic neuropathy (LHON) is a mitochondrial genetic disease that ultimately causes bilateral vision loss due to retinal ganglion cell (RGC) degeneration. The early clinical signs of LHON include the development of central scotoma and progressive visual impairment. The acute phase of the disease is characterized by optic disc congestion, peripheral telangiectasia of the retinal vasculature, vascular tortuosity and retinal nerve fiber layer (RNFL) swelling (1, 2). More than 90% cases of LHON are caused by three mitochondrial DNA (mtDNA) point mutations: m.3460G > A, m.11778G > A and m.14484 T > C. All of these mutations affect the genes encoding different subunits of NADH dehydrogenase (mitochondrial complex I) of the mitochondrial respiratory chain (3). However, many individuals carrying mtDNA mutations appear to not develop the disease (4). Such incomplete penetrance of LHON cannot be solely explained by mitochondrial genetics, other factors such as nuclear DNA genetic background and environmental influence may play important roles in the disease onset (5).

Jurkute *et al*. (6) reported that smoking and estrogen levels increased the overall risk of LHON-associated vision failure. Other reports also indicate that LHON phenotype development in monozygotic twin brothers is inconsistent, suggesting that environmental factors play a role in LHON phenotype expression (7, 8). Smoking and alcohol abuse are the cause of exposure to environmentally toxic substances that induce large amounts of reactive oxygen species (ROS). Further research has also shown that ROS accumulation caused by environmental stress associated with drug or alcohol abuse can stimulate the earlier onset of the disease (9). The studies of mtDNA-mutated cybrid cell lines revealed that LHON-causative mutations increased endogenous ROS production (10–12). Although these cell lines do not fully mimic neuronal energy metabolism due to the special morphology of nerve cells, these results suggest that exogenous or endogenous oxidative stress may play an important role in the LHON onset.

Mitochondria are the key regulators of neuronal homeostasis and profoundly affect neurodegenerative diseases such as Alzheimer's disease and Parkinson's disease. Mitochondrial retrograde signaling can communicate their biological energy status within the cells (13). RGCs are highly polarized neurons that produce axons extending to 5 cm in length from the cell soma (14). The human optic nerve fibers are characterized by extremely high density of mitochondria and high energy requirement in the unmyelinated prelaminar region, which underlie the targeting of the optic nerve by hereditary mitochondrial diseases (15). The dynamic localization of mitochondria affects the morphogenesis of nerve cells and requires sufficient energy support (16). Mitochondrial dynamics regulates mtDNA stability, mitochondrial distribution and cell death (17). Mitochondrial dynamics plays a particularly important role in cell types highly dependent on mitochondrial functions and may be an important factor in neurodegeneration of the LHON-affected optic nerve.

Neuronal axons consist of microtubules that direct mitochondrial movement from the cell soma toward the apical end (anterograde transport), and from the apical end toward the soma (retrograde transport) (18). There are two kinds of motor proteins involved in the transport of mitochondria in different directions. The first is the kinesin family of proteins that carry cargo in anterograde transport, and the other constitutes the dynein family of proteins that carry cargo in the retrograde direction (19, 20). In addition, mitochondrial transport is specifically regulated by anchor proteins (21). The kinesin-1 family member, known as KIF5, is the major motor protein that can be driven by adenosine triphosphate (ATP) and transported along the microtubules of axons (22). Furthermore, other kinesin motors such as the kinesin-3 family proteins, KIF1B and KLP6, were also found to drive anterograde mitochondrial motion (23, 24). Three members of KIF5 proteins (KIF5A, KIF5B and KIF5C) are expressed in mammals, in which KIF5B is ubiquitously expressed, while KIF5A and KIF5C are specifically expressed only in neuronal cells (25).

In this study, we provide evidence supporting the hypothesis that nuclear genetic factors and environmental factors are involved in the RGC death effects in LHON pathogenesis. We show that RGCs affected by LHON are characterized by the abnormality of mitochondrial movement along the RGC axons, by high levels of endogenous ROS, and inhibited expression of KIF5A. This results in the induction of the cell death pathway regulated by Bcl-2 family of proteins. Furthermore, RGCs derived from unaffected LHON mutation carrier had similar ROS production, but no nuclear gene factors (such as KIF5A) were involved. The novel role of KIF5A may help us to understand the mechanisms of incomplete penetrance of LHON and help the development of novel therapeutic strategies.

Results

Differentiation of hiPSCs to RGCs

In our previous study, we characterized human-induced pluripotent stem cell (hiPSC) lines derived from healthy wild-type control individual, asymptomatic m.11778 G > A mutation carrier and LHON-affected patient with the same mutation (26). In this study, these hiPSCs were used to generate RGCs as an *in vitro* disease model of LHON. RGCs were differentiated in a step-wise differentiation protocol that included the stages of embryoid bodies (EBs), neural rosettes (NRs) and optic vesicles (OVs) (Fig. 1A). Prior to differentiation into mature RGCs, the cell aggregates of OVs were disintegrated by trypsinization and passed through a strainer as was described in our previous study (27). Therefore, the homogeneous and spatially separated populations of RGCs with neuronal morphologies were obtained (Fig. 1B). As shown by immunofluorescence staining, these RGCs expressed neuron-specific cytoskeletal marker βIII tubulin (TuJ1), as well as ATOH7, RGC-specific transcription factor (Fig. 1C). Lastly, the purity of RGC population was assessed by immunostaining the surface marker THY1 and analyzing the proportion of THY1-expressing cells by flow cytometry. The results showed that the percentage of THY1 expression was 78.7% in the control group, 60.9% in the affected group and 93.2% in the unaffected group (Fig. 1B).

ROS production and apoptosis are increased in LHON-affected hiPSC-derived RGCs

Previous studies have shown that *MT-ND4* mutations lead to elevated levels of oxidative stress, which results in dysfunction of RGCs and ultimately apoptosis. Therefore, to determine the level of intracellular ROS, we stained hiPSC-derived RGCs with DCFH-DA and measured ROS levels by flow cytometry. Compared with the control RGCs, ROS production was significantly increased by 2-fold in the affected and carrier RGCs (Fig. 2A). Furthermore, by using annexin V staining on day 14 of differentiation, we found that LHON-affected RGCs were characterized by more than 10-fold increase of apoptosis, in contrast to the control cells (Fig. 2B). Notably, unaffected LHON-RGCs showed no

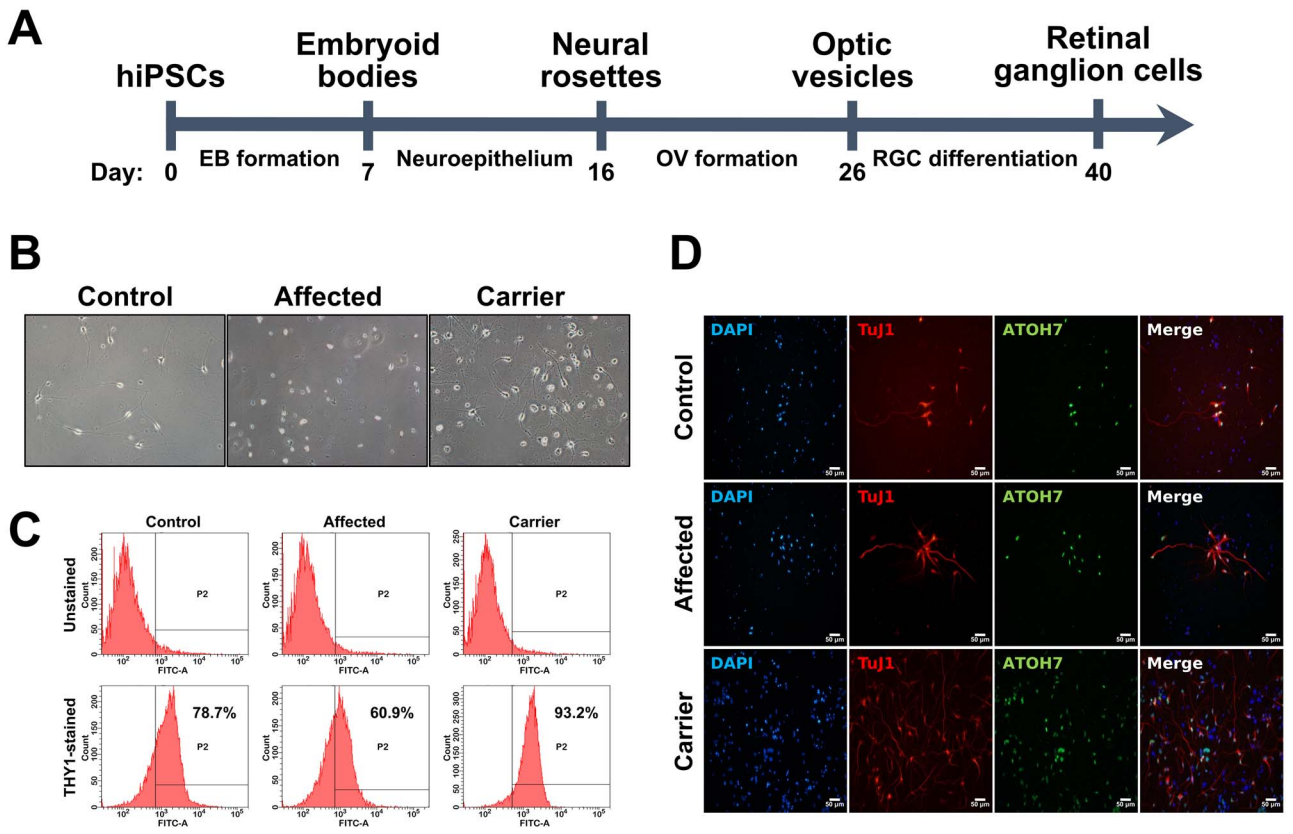

Figure 1. Differentiation of hiPSCs to RGCs. (**A**) The schematic diagram showing the timeline and intermediate stages of differentiation of hiPSCs into RGCs. (**B**) Bright field images of mature hiPSC-derived RGCs. (**C**) Flow cytometry analysis of proportion of hiPSC-derived RGCs expressing THY1 marker. (**D**) Immunostaining showing expression of RGC markers ATOH7 and TuJ1 in hiPSC-derived RGCs. Nuclei stained with DAPI.

significant increase in apoptosis (Fig. 2B). The reduction of the excessive oxygen poisoning may be one of the strategies to prevent LHON-induced loss of vision. N-acetyl-L-cysteine (NAC) is a well-known scavenger of ROS, which increases the synthesis of glutathione (28). Under the conditions used in this study, treatment with NAC for 24 h caused a decrease in intracellular ROS levels in the affected and carrier RGCs (Fig.s 2C). In addition, cells were treated with 0, 5 and 10 mM NAC for 24 h, and apoptosis was analyzed. Annexin V/PI staining showed that the apoptosis in the affected LHON-RGCs decreased after NAC treatment (Fig. 2D). This result suggests that the reduction of intracellular ROS by NAC may be beneficial for LHON hiPSC-derived RGCs.

Mitochondrial transport patterns in LHON-specific RGCs

In order to assess mitochondrial movement along the axons of control, affected and carrier hiPSC-derived RGCs, the living cells were stained with MitoTracker Red (Fig. 3A). The patterns of mitochondrial anterograde transport, retrograde transport and long-term stationary condition in axons were compared using kymographs. In control RGC axons, about 60% of the mitochondria were stationary, while the anterograde and retrograde mitochondria constituted about 20% each (Fig. 3B and C). The mitochondrial movement in carrier RGC axons was similar to that in normal cells (Fig. 3B and 3C). Interestingly, in the affected axons, retrograde mitochondrial motion increased to 40%, while stationary mitochondria decreased to 40%, and the proportion of anterograde mitochondria remained at 20% (Fig. 3B and C).

KIF5A expression is decreased in LHON-affected human RGCs

The mitochondrial migration patterns, including anterograde and retrograde transport, are the result of co-regulation of anterograde and retrograde motor proteins and docking machinery. In axons, dynein motors are responsible for retrograde movement toward the soma, while KIF5 family motors drive anterograde transport to distal axonal regions and synaptic terminals. Syntaphilin (SNPH) is an important mitochondrial docking protein that immobilizes mitochondria specifically in axons (29).

Since we observed differences in mitochondrial migration patterns in normal and LHON-specific RGCs (Fig. 3), we measured the expression levels of genes encoding different motor proteins by quantitative reverse transcription-polymerase chain reaction (qRT-PCR). The expression of messenger RNAs (mRNAs) encoding anterograde motor proteins, KIF5A and KIF5C, was significantly decreased in LHON-affected hiPSC-derived RGCs, in contrast, mRNAs encoding retrograde motor proteins, DNAH7 and DNAH17, were upregulated (Fig. 4A). Moreover, the protein expression levels of KIF5A, KIF5C and SNPH were also measured by western blot (Fig. 4B). Consistently with qRT-PCR, western blot results showed drastically decreased protein expression of KIF5A in affected RGCs, whereas SNPH level was significantly upregulated (Fig. 4C). Taken together, these results suggested that the mitochondria motor proteins were regulated in affected LHON iPSC-derived RGCs compared with the isogenic control.

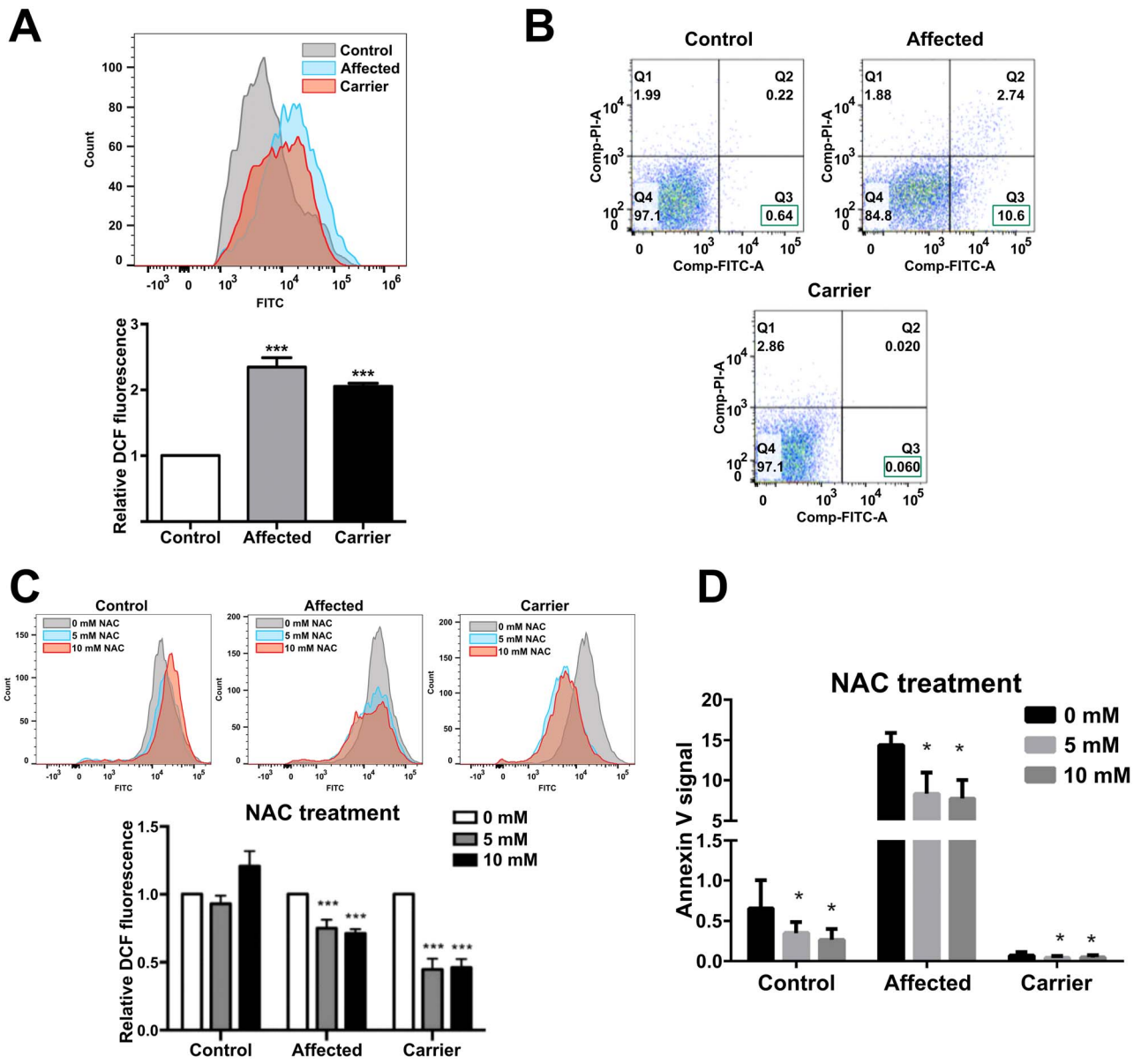

Figure 2. ROS production and apoptosis are increased in LHON-affected hiPSC-derived RGCs. (**A**) Measurement of ROS levels in hiPSC-derived RGCs by DCFH-DA staining and flow cytometry. Top panel: representative flow cytometry profile. Bottom panel: quantification of mean fluorescence in affected and carrier samples expressed as relative to control. (**B**) Flow cytometry analysis of annexin V-stained cells in hiPSC-derived RGCs. The percentage of annexin V-positive apoptotic cells shown in bottom-right corner (green rectangle). (**C**) Measurement of ROS levels in hiPSC-derived RGCs treated with the indicated concentrations of NAC by DCFH-DA staining and flow cytometry. Top panel: representative flow cytometry profiles. Bottom panel: quantification of mean fluorescence in affected and carrier samples expressed as relative to control. (**D**) Flow cytometry analysis of annexin V-stained cells in hiPSC-derived RGCs treated with the indicated concentrations of NAC. Quantitative data are expressed as means ± SD error bars, $^{*}P < 0.05$, $^{**}P < 0.01$, $^{***}P < 0.001$.

The effect of ROS on KIF5A expression and mitochondrial mobility in LHON hiPSC-derived RGCs

To determine the effect of ROS on mitochondrial mobility in LHON-specific RGCs, we observed mitochondrial movement after treating cells with NAC. The control and mutant affected and carrier hiPSC-derived RGCs were treated with 5 mM NAC for 24 h and stained with MitoTracker Red. Although NAC treatment reduced anterograde mitochondrial movement and increased resting mitochondria in control hiPSC-derived RGCs, there were still more than 60% of resting mitochondria and less than 20% of anterograde and retrograde mitochondria, respectively (Fig. 5A). However, in the affected LHON hiPSC-derived RGCs, NAC treatment significantly reduced the percentage of retrograde mitochondria to 22% and increased the proportion of stationary mitochondria by 10% (Fig. 5B). In the carrier LHON hiPSC-derived RGCs, although the NAC treatment also changed the percentage of anterograde and stationary mitochondria, the mitochondrial movement pattern was still similar to that in control RGCs (Fig. 5C). The effect of NAC on motor protein expression levels was further confirmed by western blotting. The NAC treatment caused a small increase in the protein expression of KIF5A and a decrease of KIF5C in control RGCs (Fig. 5D). Moreover, NAC treatment significantly increased the protein expression of KIF5A in the affected LHON RGCs (Fig. 5E). Furthermore, NAC had

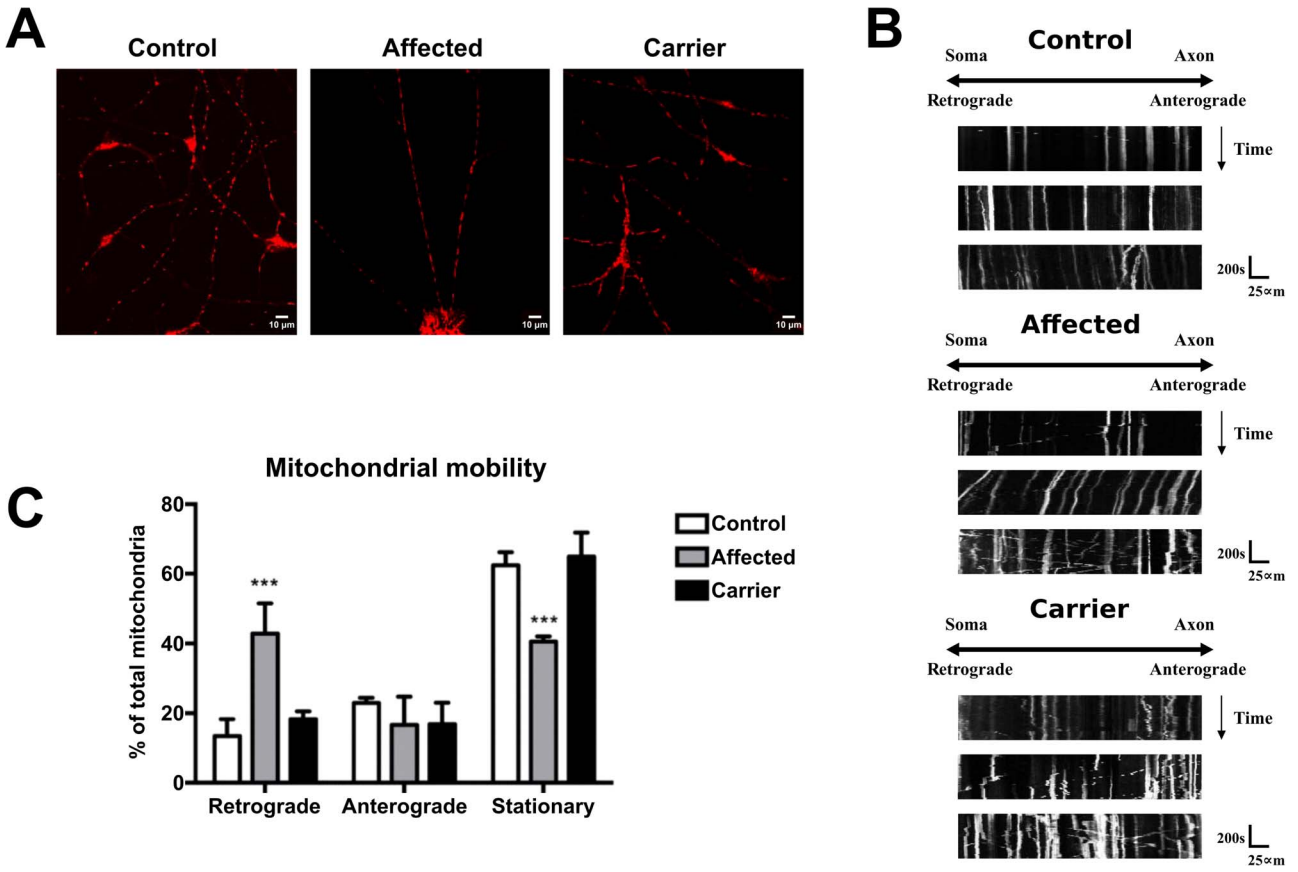

Figure 3. Mitochondrial transport patterns in LHON-specific RGCs. (**A**) Confocal microscopy images of control and LHON affected and carrier hiPSC-derived RGCs with mitochondria stained with MitoTracker Red. (**B**) Kymograph analysis of mitochondrial movement in single axons revealing the movement patterns of mitochondria. (**C**) Percentage of mitochondrial stationary, anterograde and retrograde motion states in different RGC axons. Data are shown as means ($n = 5$) ± SD error bars, $^{***}P < 0.001$ (Student's *t*-test).

no significant effect on the motor protein level in carrier RGCs (Fig. 5F). These results indicate that the ROS in the affected RGCs inhibit the protein expression of KIF5A and cause an increase in retrograde movement of the mitochondria in the axons.

KIF5A upregulates the expression of Bcl-2 in affected RGCs

To further characterize the role of KIF5A in affected RGCs, we examined the effect of KIF5A on apoptosis. Since LHON-associated apoptosis occurs via mitochondrial pathway, we tested the effect of KIF5A on crucial regulators of this pathway: antiapoptotic protein Bcl-2 and proapoptotic protein BAD. KIF5A was overexpressed in hiPSC-derived RGCs and the protein expression levels of Bcl-2 and BAD were examined by western blotting. Interestingly, overexpression of KIF5A increased the protein expression of Bcl-2 in the affected RGCs, but did not affect the protein expression of BAD. In addition, overexpression of KIF5A did not affect the expression of Bcl-2 and Bad in normal RGCs (Fig. 6A). In basal condition, the level of Bcl-2 in carrier RGCs was higher than that in normal and affected RGCs (Fig. 6A). At the same time, as was measured by annexin V staining, affected RGCs transfected with KIF5A demonstrated significantly increased proportion of apoptotic cells in comparison with the cells transfected with vector control, which was not the case for control and carrier cells (Fig. 6B).

Discussion

In normal mature axons, most of the mitochondria are long-term stationary (more than 70%), while a small proportion (less than 30%) moves in the anterograde and retrograde directions to meet long distance metabolic requirements (31). Our hiPSC-derived RGCs were similar to other mature neuronal axons, with more than 60% of long-term stationary mitochondria and less than 40% of moving in anterograde and retrograde directions (Fig. 3). LHON is one of the hereditary mitochondrial disorders and also one of the most important optic neuropathies causing severe RGC impairment and visual failure resultant from the death of RGCs. Even though the causal mutations of LHON are known today, little is known about the actual factors that potentiate its special clinical features such as incomplete penetrance, gender bias and specificity in affecting RGCs, but not other cell types (32). The mtDNA mutations are necessary, but not sufficient to cause LHON (33). There are other reasons behind the failure of RGCs, including specific transcriptional activity, environmental factors, elevated ROS production and loss of cellular energy. Here, we found that the proportion of long-term stationary mitochondria in the affected RGC axons decreased to 40%, while the retrograde mitochondria increased to 40%, and only the proportion of anterograde mitochondria remained the same as in the control RGCs (Fig. 3).

ROS production has been reported to be related to mitochondrial transport. In fact, previous studies showed that increased ROS production caused mitochondria to be dysmobilized (34).

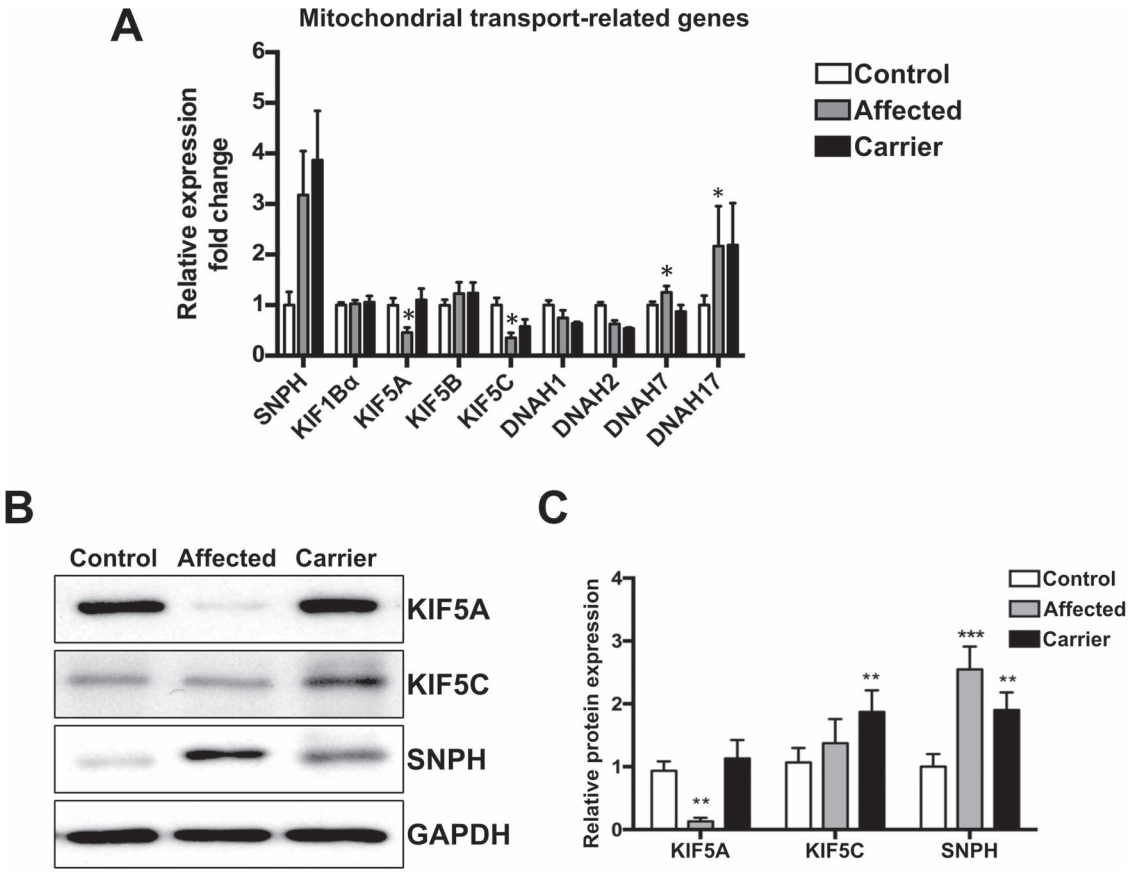

Figure 4. KIF5A expression is decreased in LHON-affected human RGCs. (**A**) qRT-PCR analysis of expression of mRNAs encoding motor proteins in control, affected and carrier hiPSC-derived RGCs. Data shown as mean fold changes from 3 biological replicates relative to control with SD error bars. $^{*}P < 0.05$ (Student's *t*-test) versus control. (**B**) Western blot analysis of endogenous KIF5A, KIF5C and SNPH protein levels in control, affected and carrier RGCs. (**C**) Quantification of expression levels of KIF5A, KIF5C and SNPH proteins measured by western blot. Data expressed as mean fold changes relative to control and normalized to GAPDH ± SD error bars, $n = 3$, $^{*}P < 0.05$, $^{**}P < 0.01$, $^{***}P < 0.001$ (Student's *t*-test).

Even drugs that are currently used to treat LHON in clinic, including Idebenone, EPI-743 and Bendavia, alleviate disease manifestation by inhibiting the production of peroxides (35). Thus, the oxidative stress is an important factor in mitochondrial disorders. In our study, we demonstrated that the levels of ROS were significantly increased in affected and carrier hiPSC-derived RGCs, in contrast to the control cells (Fig. 2). In addition, NAC, which is a scavenger of ROS, reduced the excessive ROS production. Our results also indicate that endogenous ROS production is significantly reduced by NAC treatment, which also reduces the cell death of RGCs in LHON (Fig. 2).

Mitochondrial dysfunction may cause ROS levels to increase and alter the expression of antioxidant genes (36). In previous studies, it has been shown that excessive mtDNA mutation-associated oxidative stress and damage were observed in patients with LHON.

Therefore, given the observations that the ROS levels in both types of LHON-specific RGCs were increased and the abnormal pattern of mitochondrial motility was observed in affected RGCs, we first measured the expression levels of different genes involved in mitochondrial movement (Fig. 4), and then sought to investigate the effect of ROS suppression by NAC on them (Fig. 5). *KIF5A*, encoding one of the isoforms of kinesin-1, demonstrated drastic downregulation in affected RGCs in comparison with both control and carrier RGCs, therefore, it was chosen as a primary candidate for a gene underlying the incomplete penetrance of LHON. At the same time, we observed significant upregulation of *SNPH* gene in both carrier and affected types of LHON-specific RGCs. This gene encodes SNPH, a protein responsible for mitochondria docking, therefore, the reduction of stationary mitochondria in affected cells may seem in contradiction with its overexpression. The immobilization of mitochondrial movement mediated by SNPH normally keeps mitochondria in the area that requires energy, also referred to as mitochondrial stationary pool (37). SNPH can directly bind to KIF5 proteins and stop the mitochondrial movement in response to neural activity. Such activity-dependent immobilization mechanism has previously been shown to be triggered by Ca^{2+} sensing by mitochondrial Rho GTPase 1 (MIRO1), resulting in interaction between SNPH and KIF5 and movement blockade (38). We hypothesize that although the affected cells have increased SNPH expression, lower KIF5A expression is the primary cause of the reduction of the percentage of stationary mitochondria due to the lack of supply of mitochondria from the soma to the axonal locations, where they can be fixed by SNPH in an activity-dependent manner. Although dynein motors are responsible for retrograde movement of mitochondria, only *DNAH17* demonstrated elevated expression in both affected and carrier comparing to control (Fig. 4A). Therefore, the possibility should not be excluded that the increase in retrograde movement in affected RGCs could be due to upregulation of kinesin, however, in the carrier genetic environment, the mechanism exists that keeps in check.

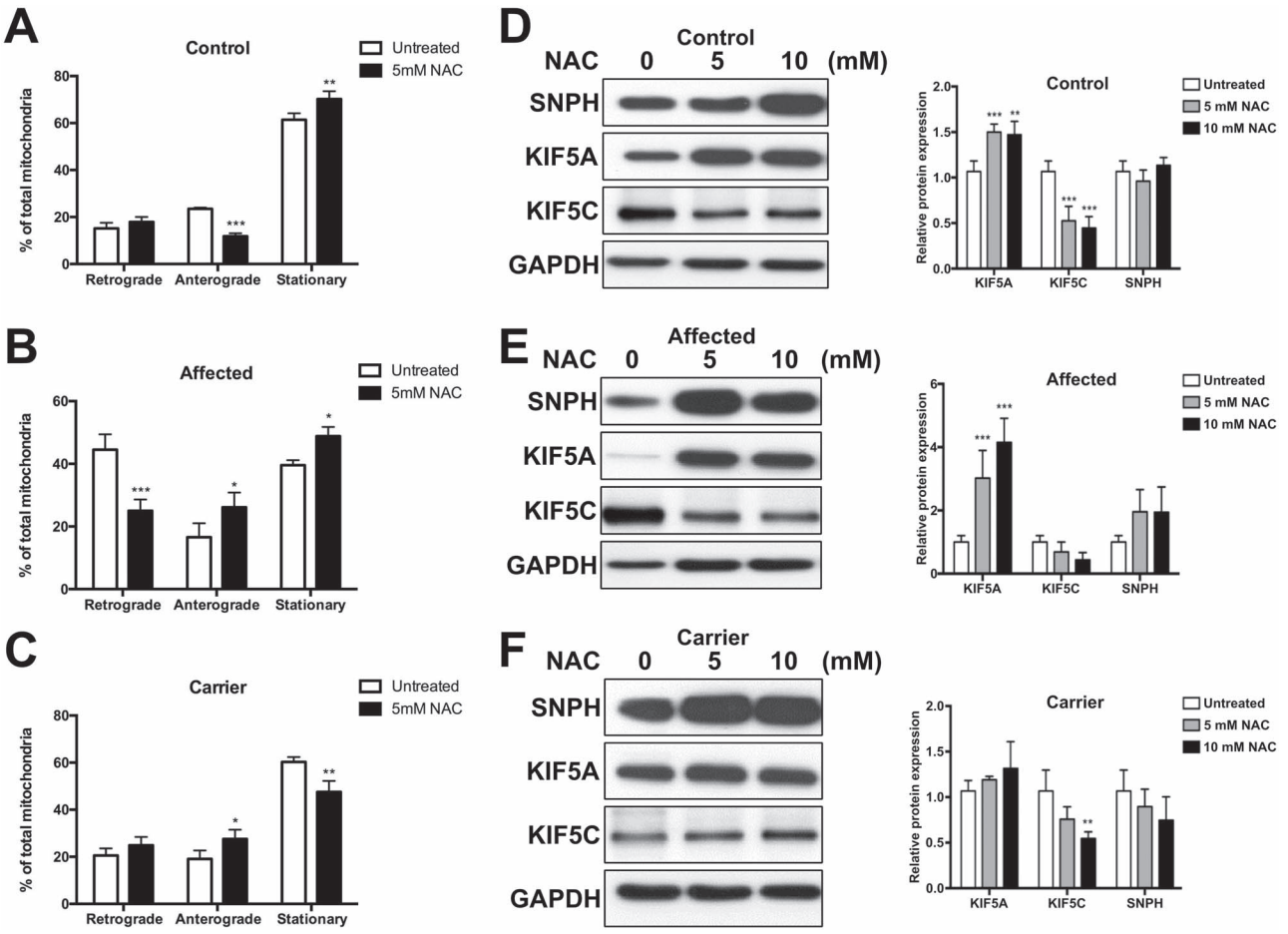

Figure 5. The effect of ROS on KIF5A expression and mitochondrial mobility in LHON hiPSC-derived RGCs. The proportions of retrograde, anterograde and stationary mitochondria in control (**A**), affected (**B**) and carrier (**C**) hiPSC-derived RGCs. Cells were treated with 5 mM NAC for 24 h, stained with MitoTracker Red and analyzed for stationary, anterograde and retrograde movement by confocal microscopy. The numbers of moving mitochondria were measured by kymograph analysis. All data represented as means ± SD, $n = 3$, $^{*}P < 0.05$, $^{**}P < 0.01$, $^{***}P < 0.001$ (Student's *t*-test). The levels of motor proteins KIF5A and KIF5C, and docking protein SNPH measured by western blotting in control (**D**), affected (**E**) and carrier (**F**) hiPSC-derived RGCs treated with the indicated concentrations of NAC. Quantification of western blot signal (right panel) shown as means ± SD, $n = 3$, $^{**}P < 0.01$, $^{***}P < 0.001$ (Student's *t*-test).

Our results indicate that both carrier and affected types of LHON-specific RGCs produce high levels of ROS (Fig. 2A), however, only affected cells were characterized by decreased level of ROS-dependent KIF5A expression (Figs 4 and 5), and, at the same time, the increased levels of apoptosis (Fig. 2B), which may be indicative of an important role of KIF5A in neuronal survival in LHON-specific genetic environment.

Indeed, in some hereditary neurological diseases, mutations in *KIF5A* gene were found to affect the axonal transport and affect the survival of neurons (39, 40). In addition, the clinical report of Duis *et al*. (41) also suggested that *KIF5A* mutations affect a wide range of phenotypes, including optic nerve abnormalities. KIF5A mutations were also found to be associated with axonal degeneration in many neurodegenerative diseases. These reports show that the expression level of KIF5A in nerve cells is regulated by environmental stresses, such as nitric oxide and protein accumulation. These stress factors downregulate KIF5A and cause neurodegeneration (42, 43). Our results show that affected RGCs are characterized by high oxidative stress that downregulates KIF5A expression, which results if increased levels of apoptosis. Some previous studies have shown several unique features of KIF5A. KIF5A mutations in zebrafish show that it plays a role in maintaining mitochondrial density and in long-range transport in the axons (44). KIF5A conditionally mutated mice were characterized by the accumulation of neurofilaments and the loss of large caliber axons (45). The same report also shows that KIF5A plays a role in microtubule-dependent slowing of axonal transport and that dorsal root ganglion sensory neurons are more affected than motor neurons (45). These results suggest that high-level ROS in affected RGCs downregulates the expression of KIF5A, which in turn affects the movements of mitochondria in axons, while KIF5A in carrier RGCs is not affected by ROS, which may be conditioned by other nuclear genes implicated in mitochondrial dynamics (46). *MT-ND4* mutations affect mitochondrial oxidative phosphorylation (OXPHOS) and ATP (47), while downregulation of KIF5A may cause abnormal distribution of axonal mitochondria or may cause loss of neurofilament transport. This also shows that the combined effect of downregulation of KIF5A expression and *MT-ND4* mutation may be a positive factor for the apoptosis of affected RGCs.

In the disease model based on LHON cybrid cells, the release of cytochrome *c* from mitochondria was clearly observed, which resulted in ROS-induced apoptosis. Apoptosis caused by cytochrome *c* release is mediated by death-promoting members of the Bcl-2 family of proteins such as BAX, BID, BAD, BAK,

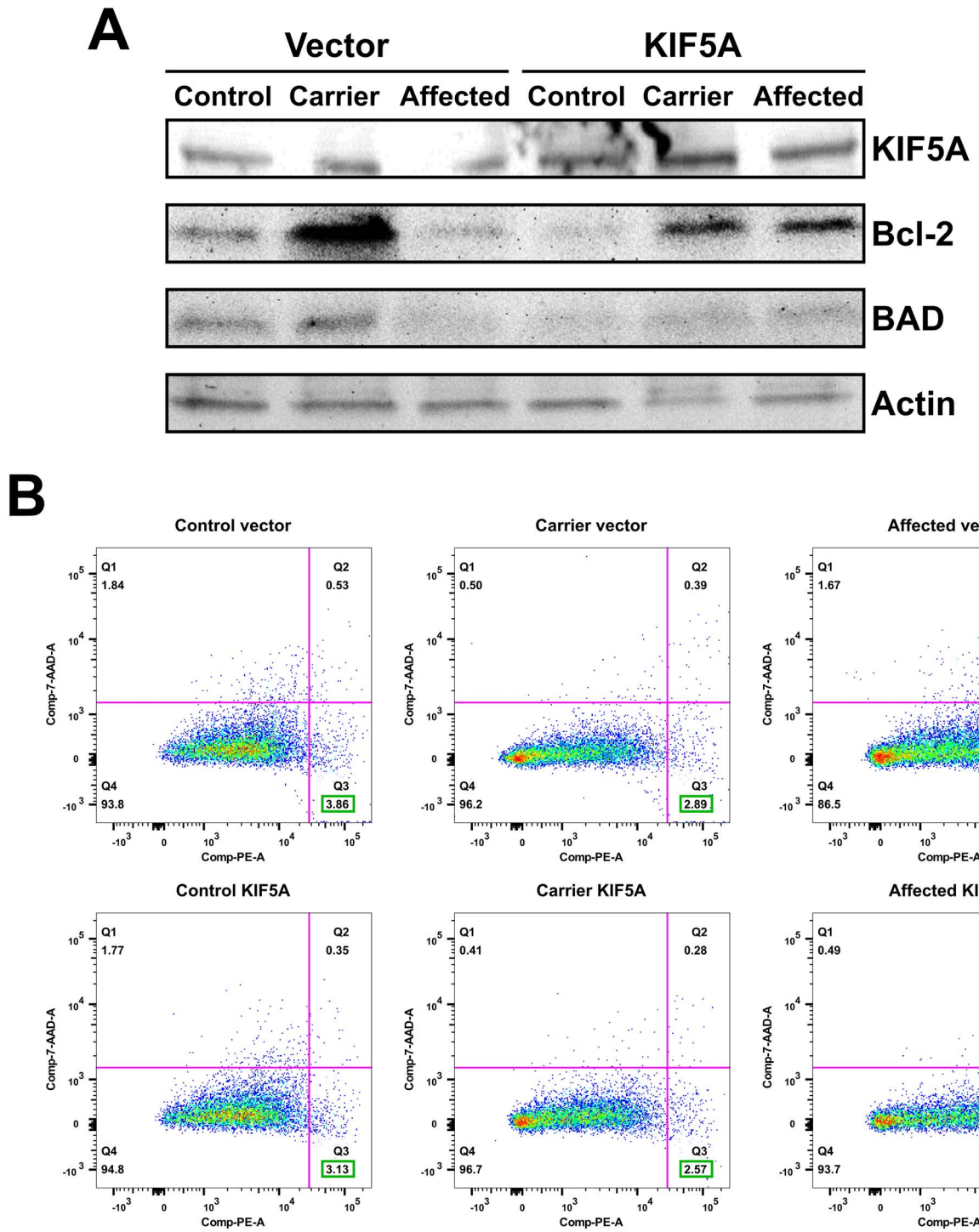

Figure 6. KIF5A upregulates the expression of Bcl-2 in affected RGCs. (**A**) KIF5A-encoding plasmid the control vector were transfected into control, carrier and affected RGCs and the levels of Bcl-2 and BAD were analyzed by western blotting. Actin used as a loading control. (**B**) Flow cytometry analysis of annexin V-stained cells in control, carrier and affected RGCs transfected with control vector and KIF5A. The percentage of annexin V-positive apoptotic cells shown in bottom-right corner (green rectangle).

BOK, but in LHON cybrid cells, the expression of BAX was not detected (48). Our results show that both BAD and Bcl-2 are detected in both mtDNA 11 778 G > A-mutated RGC lines (affected and carrier), indicating that these RGCs may be in apoptosis-sensitive state. Overexpression of KIF5A may help to increase pro-survival gene expression in affected RGCs, such as Bcl-2, which shows possible ways to help LHON RGCs survive and show possible clinical diagnostic markers. mtDNA 11 778 G > A causes RGC to produce more ROS, and in addition, the expression of KIF5A is reduced in affected LHON RGCs. These abnormal factors cause changes in the mitochondrial movement pattern. Abnormal mitochondrial movement is associated with

Table 1. Sequences of the primer used for qPCR analysis

Gene name	Forward primer sequence	Reverse primer sequence
GAPDH	GTCGCCAGCCGAGCCACATC	CCAGGCGCCCAATACGACCA
SNPH	TGGAAGAGGAGGAGGAGGCT	ACCACCACAGCCAGCAGATC
KIF5A	GCCTCTTCCAGAACTACCAGAATC	CCATTGTCCATGTTGGCCTT
KIF5B	ATGCAGATCTCCGCTGTGAACT	AGCGTTTGCGATCACGAGAT
KIF5C	ACTCTTTGTCCAGGATCTGACCAC	GGACCAGCTGCTTGTGAACTTT
KIF1B	CGATGAAGCAAGGAAAGGGA	GCTGCTTGCTAACTTGGATGTG
DNAH1	CTGTACACAGAGATGGCCGTTATC	GTTGGTAGAGTGTCCTGTGGTTGA
DNAH2	CACTGACAGACCTAGAGAAAGGCA	GGAGGAACATGGGCATCAAA
DNAH7	GATGTGGCTAAAGCCCTGTAAGAG	GAGGGAAGAGTCATGGCAATCA
DNAH17	TCCTACGTGTACGGACTCTTCATG	TCCACAGGAATGGCCTTGAT

several neurodegenerative diseases (29, 49) and also affects optic atrophy in LHON patients.

Materials and Methods

Differentiation of RGCs from hiPSCs

RGC-containing OVs were produced from hiPSCs as previously described (30). Single RGCs were separated from RGC-containing OVs by treatment with TrypLE (Thermo Fisher Scientific, Waltham, MA, USA) for 5 min at 37°C. The single RGC were then cultured on a cell culture dish coated with poly-D-lysine and laminin in DMEM/F12 medium containing N-2 supplement (Gibco, Carlsbad, CA, USA), on the following day the medium was replaced with Neurobasal medium/B27 (Gibco) supplemented with DAPT. On days 14–16, neurite outgrowth of the single RGCs could be observed.

Immunofluorescence staining

Cells on coverslips were fixed in 75% ethanol for 24 h at 4°C and rinsed with phosphate-buffered saline (PBS), then permeabilized by treatment with 0.1% NP-40 in PBS for 20 min. Then, cells were washed in PBS twice, blocked with 5% FBS in PBS for 10 min three times, and incubated with primary antibodies for 24 h at 4°C. The primary antibodies (1:100) used in this study included anti-ATOH7 (Cell Signaling Technology, Danvers, MA, USA), anti-beta III tubulin (Abcam, Cambridge, UK), anti-BRN3B (Cell Signaling Technology), anti-THY1 (Cell Signaling Technology) and anti-beta III tubulin (Cell Signaling Technology). After incubation with primary antibodies, cells were washed three times with PBS. Secondary antibodies (1:200) were applied for 1 h at room temperature. Nuclei were stained with DAPI (1:8000) for 10 min. Then, after washing with PBS three times, cells were mounted on slides with mounting solution. Slides were then examined on FV10i laser confocal microscope (Olympus, Tokyo, Japan).

Measurement of ROS

The intracellular ROS level was measured by staining with 5 μM DCFH-DA at 37°C for 30 min. The fluorescence intensity of 1×10^5 cells was analyzed using the BD FACSCalibur flow cytometer.

Detection of apoptosis

Apoptosis events were determined by FITC Annexin V Apoptosis Detection Kit I (BD Biosciences, San Jose, CA, USA) according to the manufacturer's instructions. For flow cytometry, cells were harvested and stained with both annexin V and PI for 10 min. The cells were washed by PBS and resuspended in 1X Binding Buffer. Then, each sample was analyzed on a BD FACSCanto II flow cytometer (BD Biosciences) within 1 h.

qRT-PCR

Total RNA was extracted by TRIzol reagent (Thermo Fisher Scientific), and complementary DNA (cDNA) was synthesized using SuperScript III Reverse Transcriptase (Thermo Fisher Scientific) using random hexamer priming. qRT-PCR reactions were performed on a 7900HT Fast Real-Time PCR System (Applied Biosystems, Foster City, CA, USA) using Power SYBR Green PCR Master Mix (Applied Biosystems). The gene-specific primer sequences are presented in Table 1.

Analysis of mitochondrial movement in axons

To visualize mitochondrial transport in hiPSC-derived RGCs, live cells growing on culture dishes were stained directly with 50 nM MitoTracker Red FM dye (Life Technologies, Carlsbad, CA, USA) for 15 min at 37°C in a 5% CO2 incubator and examined using FV10i laser confocal microscope (Olympus). Time-lapse imaging was performed using a confocal microscope. All movies were processed and analyzed using ImageJ software. Kymographs were used to quantify relative mitochondrial mobility. Using kymographs, the numbers of mitochondria moving in anterograde and retrograde directions were quantified along with the number of stationary mitochondria.

Western blotting

Cell was lysed on ice in RIPA lysis buffer (Thermo Fisher Scientific) containing, 1% protease inhibitor. The protein blots were blocked with 0.5% skimmed milk and 0.3% bovine serum albumin (Sigma-Aldrich, St. Louis, MO, USA) in PBS for 1 h and then incubated with antibodies against KIF5A (1: 1000; Proteintech, Rosemont, IL, USA), KIF5C (1: 1000; Proteintech), SNPH (1: 1000; Abcam), GAPDH (1: 5000; Cell Signaling), Bcl-2 (1: 1000; Cell Signaling), BAD (1: 1000; Cell Signaling) and β-tubulin (1: 5000, Cell Signaling) at 4°C overnight. The blots were then washed with PBS and incubated for 2 h at room temperature with 1: 2000 diluted horseradish peroxidase-conjugated anti-mouse or rabbit IgG antibodies (Cell Signaling). The blots were then visualized using an enhanced chemiluminescence detection system.

Statistical analysis

The quantifiable data are presented as the means from at least three biological replicates with standard deviation error bars.

The data were compared using Student's *t*-test, with at least $P < 0.05$ considered as statistically significant.

Funding

This study was funded by The Ministry of Science and Technology (MOST 106-2633-B-009-001, MOST106-2119-M-010-001, MOST106-2319-B-001-003, MOST106-3114-B-010-002, MOST 107-2119-M-010-001, MOST 107-2633-B-009-003, MOST107-2321-B-010-007, MOST107-2320-B-010-023, and MOST 107-2319-B-001-003); Academia Sinica and Ministry of Science and Technology (106-0210-01-15-02 and 107-0210-01-19-01); Academia Sinica (VTA107-V1-5-1 and VTA108-V1-5-3); the Ministry of Health and Welfare (MOHW)(106-TDU-B-211-113001, 107-TDU-B-211-123001 and 108-TDU-B-211-133001); National Health Research Institutes (NHRI) (EX106-AQ8 10621BI, EX107-10621BI and EX108-10621BI);Taipei Veterans General Hospital (V106C-001, V107C-139, V107E-002-2, 108E-002-2, and V108D46-004-MY2-1); Taipei Veterans General Hospital (TVGH) and National Taiwan University Hospital (NTU) Joint Project (VN106-02, VN107-16 and VN108-15); Veterans General Hospital (VGH), Tri-Service General Hospital (TSGH), National Defense Medical Center (NDMC), Academia Sinica (AS) Joint Research Program (VTA107/108-V1-5-1); Excellent Clinical Trail Center (MOHW106-TDU-B-211-113001, MOHW 107-TDU-B-211-123001, MOHW108-TDU-B-211-133001); the Ministry of Education (particularly supported through the SPROUT Project: the "Center for Intelligent Drug Systems and Smart Bio-devices (IDS2B)" of National Chiao Tung University in Taiwan); the "Cancer Progression Research Center; and National Yang-Ming University (from The Featured Areas Research Center Program within the framework of the Higher Education Sprout Project by the Ministry of Education (MOE)" in Taiwan).

Conflict of Interest Statement. The authors declare no conflict of interest.

References

1. La Morgia, C., Carbonelli, M., Barboni, P., Sadun, A.A. and Carelli, V. (2014) Medical management of hereditary optic neuropathies. *Front. Neurol.*, **5**, 141.
2. Meyerson, C., Van Stavern, G. and McClelland, C. (2015) Leber hereditary optic neuropathy: current perspectives. *Clin. Ophthalmol.*, **9**, 1165–1176.
3. Yu-Wai-Man, P., Griffiths, P.G., Hudson, G. and Chinnery, P.F. (2009) Inherited mitochondrial optic neuropathies. *J. Med. Genet.*, **46**, 145–158.
4. Howell, N. and Mackey, D.A. (1998) Low-penetrance branches in matrilineal pedigrees with Leber hereditary optic neuropathy. *Am. J. Hum. Genet.*, **63**, 1220–1224.
5. Caporali, L., Maresca, A., Capristo, M., Del Dotto, V., Tagliavini, F., Valentino, M.L., La Morgia, C. and Carelli, V. (2017) Incomplete penetrance in mitochondrial optic neuropathies. *Mitochondrion*, **36**, 130–137.
6. Jurkute, N. and Yu-Wai-Man, P. (2017) Leber hereditary optic neuropathy: bridging the translational gap. *Curr. Opin. Ophthalmol.*, **28**, 403–409.
7. Biousse, V., Brown, M.D., Newman, N.J., Allen, J.C., Rosenfeld, J., Meola, G. and Wallace, D.C. (1997) De novo 14484 mitochondrial DNA mutation in monozygotic twins discordant for Leber's hereditary optic neuropathy. *Neurology*, **49**, 1136–1138.
8. Johns, D.R., Smith, K.H., Miller, N.R., Sulewski, M.E. and Bias, W.B. (1993) Identical twins who are discordant for Leber's hereditary optic neuropathy. *Arch. Ophthalmol.*, **111**, 1491–1494.
9. Kogachi, K., Ter-Zakarian, A., Asanad, S., Sadun, A. and Karanjia, R. (2019) Toxic medications in Leber's hereditary optic neuropathy. *Mitochondrion*, **46**, 270–277.
10. Giordano, C., Montopoli, M., Perli, E., Orlandi, M., Fantin, M., Ross-Cisneros, F.N., Caparrotta, L., Martinuzzi, A., Ragazzi, E., Ghelli, A. *et al.* (2011) Oestrogens ameliorate mitochondrial dysfunction in Leber's hereditary optic neuropathy. *Brain*, **134**, 220–234.
11. Floreani, M., Napoli, E., Martinuzzi, A., Pantano, G., De Riva, V., Trevisan, R., Bisetto, E., Valente, L., Carelli, V. and Dabbeni-Sala, F. (2005) Antioxidant defences in cybrids harboring mtDNA mutations associated with Leber's hereditary optic neuropathy. *FEBS J.*, **272**, 1124–1135.
12. Giordano, L., Deceglie, S., d'Adamo, P., Valentino, M.L., La Morgia, C., Fracasso, F., Roberti, M., Cappellari, M., Petrosillo, G., Ciaravolo, S. *et al.* (2015) Cigarette toxicity triggers Leber's hereditary optic neuropathy by affecting mtDNA copy number, oxidative phosphorylation and ROS detoxification pathways. *Cell Death Dis.*, **6**, e2021.
13. Cagin, U., Duncan, O.F., Gatt, A.P., Dionne, M.S., Sweeney, S.T. and Bateman, J.M. (2015) Mitochondrial retrograde signaling regulates neuronal function. *Proc. Natl. Acad. Sci. U. S. A.*, **112**, E6000–E6009.
14. Curcio, C.A. and Allen, K.A. (1990) Topography of ganglion cells in human retina. *J. Comp. Neurol.*, **300**, 5–25.
15. Barron, M.J. (2004) The distributions of mitochondria and sodium channels reflect the specific energy requirements and conduction properties of the human optic nerve head. *Br. J. Ophthalmol.*, **88**, 286–290.
16. Li, Z., Okamoto, K., Hayashi, Y. and Sheng, M. (2004) The importance of dendritic mitochondria in the morphogenesis and plasticity of spines and synapses. *Cell*, **119**, 873–887.
17. Van Laar, V.S., Arnold, B., Howlett, E.H., Calderon, M.J., St Croix, C.M., Greenamyre, J.T., Sanders, L.H. and Berman, S.B. (2018) Evidence for compartmentalized axonal mitochondrial biogenesis: mitochondrial DNA replication increases in distal axons as an early response to Parkinson's disease-relevant stress. *J. Neurosci.*, **38**, 7505–7515.
18. Baas, P.W. and Lin, S. (2011) Hooks and comets: the story of microtubule polarity orientation in the neuron. *Dev. Neurobiol.*, **71**, 403–418.
19. Huang, C.F. and Banker, G. (2012) The translocation selectivity of the kinesins that mediate neuronal organelle transport. *Traffic*, **13**, 549–564.
20. Kapitein, L.C., Schlager, M.A., Kuijpers, M., Wulf, P.S., van Spronsen, M., MacKintosh, F.C. and Hoogenraad, C.C. (2010) Mixed microtubules steer dynein-driven cargo transport into dendrites. *Curr. Biol.*, **20**, 290–299.
21. Cai, Q. and Sheng, Z.H. (2009) Mitochondrial transport and docking in axons. *Exp. Neurol.*, **218**, 257–267.
22. Pilling, A.D., Horiuchi, D., Lively, C.M. and Saxton, W.M. (2006) Kinesin-1 and dynein are the primary motors for fast transport of mitochondria in drosophila motor axons. *Mol. Biol. Cell*, **17**, 2057–2068.
23. Nangaku, M., Sato-Yoshitake, R., Okada, Y., Noda, Y., Takemura, R., Yamazaki, H. and Hirokawa, N. (1994) KIF1B, a novel microtubule plus end-directed monomeric motor protein for transport of mitochondria. *Cell*, **79**, 1209–1220.
24. Tanaka, K., Sugiura, Y., Ichishita, R., Mihara, K. and Oka, T. (2011) KLP6: a newly identified kinesin that regulates the morphology and transport of mitochondria in neuronal cells. *J. Cell Sci.*, **124**, 2457–2465.

25. Campbell, P.D. and Marlow, F.L. (2013) Temporal and tissue specific gene expression patterns of the zebrafish kinesin-1 heavy chain family, kif5s, during development. *Gene Expr. Patterns*, **13**, 271–279.
26. Wu, Y.R., Wang, A.G., Chen, Y.T., Yarmishyn, A.A., Buddhakosai, W., Yang, T.C., Hwang, D.K., Yang, Y.P., Shen, C.N., Lee, H.C. *et al.* (2018) Bioactivity and gene expression profiles of hiPSC-generated retinal ganglion cells in MT-ND4 mutated Leber's hereditary optic neuropathy. *Exp. Cell Res.*, **363**, 299–309.
27. Yang, Y.P., Nguyen, P.N.N., Lin, T.C., Yarmishyn, A.A., Chen, W.S., Hwang, D.K., Chiou, G.Y., Lin, T.W., Chien, C.S., Tsai, C.Y. *et al.* (2019) Glutamate stimulation dysregulates AMPA receptors-induced signal transduction pathway in Leber's inherited optic neuropathy patient-specific hiPSC-derived retinal ganglion cells. *Cell*, **8**, 625.
28. Shimamoto, K., Hayashi, H., Taniai, E., Morita, R., Imaoka, M., Ishii, Y., Suzuki, K., Shibutani, M. and Mitsumori, K. (2011) Antioxidant N-acetyl-L-cysteine (NAC) supplementation reduces reactive oxygen species (ROS)-mediated hepatocellular tumor promotion of indole-3-carbinol (I3C) in rats. *J. Toxicol. Sci.*, **36**, 775–786.
29. Sheng, Z.H. and Cai, Q. (2012) Mitochondrial transport in neurons: impact on synaptic homeostasis and neurodegeneration. *Nat. Rev. Neurosci.*, **13**, 77–93.
30. Yang, T.C., Chuang, J.H., Buddhakosai, W., Wu, W.J., Lee, C.J., Chen, W.S., Yang, Y.P., Li, M.C., Peng, C.H. and Chen, S.J. (2017) Elongation of axon extension for human iPSC-derived retinal ganglion cells by a Nano-imprinted scaffold. *Int. J. Mol. Sci.*, **18**, 2013.
31. Misgeld, T., Kerschensteiner, M., Bareyre, F.M., Burgess, R.W. and Lichtman, J.W. (2007) Imaging axonal transport of mitochondria in vivo. *Nat. Methods*, **4**, 559–561.
32. Tonska, K., Kodron, A. and Bartnik, E. (2010) Genotype-phenotype correlations in Leber hereditary optic neuropathy. *Biochim. Biophys. Acta*, **1797**, 1119–1123.
33. Carelli, V., Giordano, C. and d'Amati, G. (2003) Pathogenic expression of homoplasmic mtDNA mutations needs a complex nuclear–mitochondrial interaction. *Trends Genet.*, **19**, 257–262.
34. Melo, T.Q., van Zomeren, K.C., Ferrari, M.F., Boddeke, H.W. and Copray, J.C. (2017) Impairment of mitochondria dynamics by human A53T alpha-synuclein and rescue by NAP (davunetide) in a cell model for Parkinson's disease. *Exp. Brain Res.*, **235**, 731–742.
35. Manickam, A.H., Michael, M.J. and Ramasamy, S. (2017) Mitochondrial genetics and therapeutic overview of Leber's hereditary optic neuropathy. *Indian J. Ophthalmol.*, **65**, 1087–1092.
36. Zhuo, Y., Luo, H. and Zhang, K. (2012) Leber hereditary optic neuropathy and oxidative stress. *Proc. Natl. Acad. Sci. U. S. A.*, **109**, 19882–19883.
37. Kang, J.S., Tian, J.H., Pan, P.Y., Zald, P., Li, C., Deng, C. and Sheng, Z.H. (2008) Docking of axonal mitochondria by syntaphilin controls their mobility and affects short-term facilitation. *Cell*, **132**, 137–148.
38. Chen, Y. and Sheng, Z.H. (2013) Kinesin-1-syntaphilin coupling mediates activity-dependent regulation of axonal mitochondrial transport. *J. Cell Biol.*, **202**, 351–364.
39. Nakajima, K., Yin, X., Takei, Y., Seog, D.H., Homma, N. and Hirokawa, N. (2012) Molecular motor KIF5A is essential for GABA(a) receptor transport, and KIF5A deletion causes epilepsy. *Neuron*, **76**, 945–961.
40. Reid, E., Kloos, M., Ashley-Koch, A., Hughes, L., Bevan, S., Svenson, I.K., Graham, F.L., Gaskell, P.C., Dearlove, A., Pericak-Vance, M.A. *et al.* (2002) A kinesin heavy chain (KIF5A) mutation in hereditary spastic paraplegia (SPG10). *Am. J. Hum. Genet.*, **71**, 1189–1194.
41. Duis, J., Dean, S., Applegate, C., Harper, A., Xiao, R., He, W., Dollar, J.D., Sun, L.R., Waberski, M.B., Crawford, T.O. *et al.* (2016) KIF5A mutations cause an infantile onset phenotype including severe myoclonus with evidence of mitochondrial dysfunction. *Ann. Neurol.*, **80**, 633–637.
42. Redondo, J., Hares, K., Wilkins, A., Scolding, N. and Kemp, K. (2015) Reductions in kinesin expression are associated with nitric oxide-induced axonal damage. *J. Neurosci. Res.*, **93**, 882–892.
43. Wang, Q., Tian, J., Chen, H., Du, H. and Guo, L. (2019) Amyloid beta-mediated KIF5A deficiency disrupts anterograde axonal mitochondrial movement. *Neurobiol. Dis.*, **127**, 410–418.
44. Campbell, P.D., Shen, K., Sapio, M.R., Glenn, T.D., Talbot, W.S. and Marlow, F.L. (2014) Unique function of Kinesin Kif5A in localization of mitochondria in axons. *J. Neurosci.*, **34**, 14717–14732.
45. Xia, C.H., Roberts, E.A., Her, L.S., Liu, X., Williams, D.S., Cleveland, D.W. and Goldstein, L.S. (2003) Abnormal neurofilament transport caused by targeted disruption of neuronal kinesin heavy chain KIF5A. *J. Cell Biol.*, **161**, 55–66.
46. Del Dotto, V., Ullah, F., Di Meo, I., Magini, P., Gusic, M., Maresca, A., Caporali, L., Palombo, F., Tagliavini, F., Baugh, E.H. *et al.* (2020) SSBP1 mutations cause mtDNA depletion underlying a complex optic atrophy disorder. *J. Clin. Invest.*, **130**, 108–125.
47. Kirches, E. (2011) LHON: mitochondrial mutations and more. *Curr. Genomics*, **12**, 44–54.
48. Ghelli, A., Zanna, C., Porcelli, A.M., Schapira, A.H., Martinuzzi, A., Carelli, V. and Rugolo, M. (2003) Leber's hereditary optic neuropathy (LHON) pathogenic mutations induce mitochondrial-dependent apoptotic death in transmitochondrial cells incubated with galactose medium. *J. Biol. Chem.*, **278**, 4145–4150.
49. Correia, S.C., Perry, G. and Moreira, P.I. (2016) Mitochondrial traffic jams in Alzheimer's disease - pinpointing the roadblocks. *Biochim. Biophys. Acta*, **1862**, 1909–1917.